ELSEVIER

Marine Chemistry 77 (2002) 93–108

MARINE CHEMISTRY

www.elsevier.com/locate/marchem

# Validated methods for sampling and headspace analysis of carbon monoxide in seawater

Huixiang Xie [a,1], Steven S. Andrews [b,2], William R. Martin [b], Jared Miller [b,3], Lori Ziolkowski [b,4], Craig D. Taylor [c], Oliver C. Zafiriou [b,*]

[a] *Institut des sciences de la mer Rimouski 310, allēe des Ursulines Rimouski, Quēbec, Canada G5L 3A1*
[b] *Department of Marine Chemistry and Geochemistry, Woods Hole Oceanographic Institution, Woods Hole, MA 02543, USA*
[c] *Biology Department, Woods Hole Oceanographic Institution, Woods Hole, MA 02543, USA*

Received 18 October 2000; received in revised form 12 March 2001; accepted 9 August 2001

**Abstract**

A headspace analysis system with well demonstrated precision and accuracy for measuring carbon monoxide (CO) in natural waters and for CO incubation experiments is described. High water/gas volume ratios are accurately set by injecting known volumes of CO-free air into known volumes of water in glass syringes. CO in equilibrated headspace gas is separated chromatographically and quantified by a mercuric oxide reduction detector. A water/gas ratio of ~ 7 is sensitive and precise enough for determining low-level CO; sensitivity can be increased by raising the water/gas ratio. At a water/gas ratio of 7 (40 ml total), the analytical blank, precision, and accuracy are 0.02 nM (nanomolar), ± 0.018 nM ± 2%, and better than ± 10%, respectively. Recovery of CO from the water phase is ~ 88%. The system is efficient, simple, convenient, rapid and robust; it responds linearly up to ~ 12 nM, and can process ~ 8–12 samples/h. Several applications are illustrated: studies elucidating subtle CO-contamination artifacts, microbial oxidation incubations, and an oceanic profile. Validated low-contamination sampling methods are presented, and contamination control measures are recommended. A detailed 0–200-m profile at BATS in summer shows less "deep" CO than previously reported, but there is CO well below the seasonal mixed layer (ML) and even at the 1% light level. 

*Keywords:* Gas analysis; Carbon monoxide; Headspace analysis; Incubations; Contamination

## 1. Introduction

Oceanic carbon monoxide (CO) has long been of biogeochemical interest because of its key role in regulating the atmospheric concentration of hydroxyl radicals (Thompson, 1992; Derwent, 1995) and because the ocean exhibits large, highly variable CO supersaturations (e.g. Conrad et al., 1982; Bates et al., 1995; Ohta et al., 1999). The large variability in upper-ocean CO concentration ([CO]) is primarily due to a pronounced diurnal cycle attributable to its

* Corresponding author. Fax: +1-508-457-2164.
*E-mail address:* ozafiriou@whoi.edu (O.C. Zafiriou).
[1] Now at The US Environmental Protection Agency, National Exposure Research Laboratory, Ecosystems Research Division, Athens, GA 30605, USA.
[2] Now at Chemistry Department, Stanford University, Stanford, CA 94305, USA.
[3] Now at Middlebury College, Middlebury, VT 05753, USA.
[4] Now at Department of Oceanography, Dalhousie University, Halifax, Nova Scotia, Canada B3H 4J1.

0304-4203/02/$ - see front matter 
PII: S0304-4203(01)00065-2

photoproduction and losses by rapid microbial uptake and gas exchange (Conrad et al., 1982; Jones, 1991; Doney et al., 1995; Najjar et al., 1995). This large variability and a factor of two uncertainty in gas exchange coefficients (Bates et al., 1995) has permitted the major aspects of CO cycling to be explored productively with sampling and analysis methods of moderate reproducibility and little-studied precision and accuracy.

Recently, it has also become clear that such short-lived photoproducts as CO also present excellent opportunities to study quantitatively the couplings among upper ocean optics and photoprocesses, microbial, chemical and gas exchange losses, and upper-ocean mixing dynamics, (Kettle, 1994; Kettle et al., 1994; Doney et al., 1995; Najjar et al., 1995; Gnanadesikan, 1996; Johnson and Bates, 1996). However, realizing this expectation depends crucially on the ability to generate high-resolution data sets of well characterized precision and accuracy, so that model–data discrepancies are identifiable with confidence and sensitivity. There is thus a need for analytical and sampling methods which are well characterized, rapid, convenient, and robust enough to permit generation of high-resolution datasets at sea, sometimes under adverse conditions (CO samples cannot be stored). Here, we present and characterize one such method, and illustrate some of its applications. Our method is based on the traditional headspace analysis of dissolved gases in aqueous solutions: extraction of CO into a headspace followed by chromatographic separation and mercuric oxide detection. Although headspace analysis of CO is not a new technique, published papers in this area rarely document either the details of the analytical precision and accuracy, or the construction and operation of their apparatus (Bullister et al., 1982; Schmidt and Conrad, 1993; Valentine and Zepp, 1993; Bourbonniere et al., 1997; Ohta, 1997). Using our method, we found that better samplers and sampling are also necessary, primarily because many plastics and elastomers emit CO at significant, varying rates that are partly dependent on their light history. These materials are nearly unavoidable in commonly used valves and sampling devices. The purpose of this paper is to document our procedures and to publish a user's guide to the many tricky factors that others have not yet demonstrated mastering in sampling and headspace analysis of CO.

## 2. Analytical method and procedure

### 2.1. Sampling

Water samples are drawn from bottle-type samplers under dim light into clean syringes, generally in duplicate with minimal delay. Syringes used were 50-ml (Perfektum®, with cemented metal Luer-Lock® tips) and 100-ml glass-only (Star™) Luer-tip. Both are fitted with three-way Nylon valves, V4 in Fig. 1C,D (Kontes Glass 420163-4503) or equivalent. The male Luer tip of V4 fits snugly into some bottle outlets and into thick-walled 0.25-in. (o.d.) Teflon tubing. If required for a tight fit, 1–3-cm lengths of such tubing are butt-sealed to water sampler outlets using minimal amounts of translucent Si tubing; if necessary, the outer Luer-lock shell of the valve is removed for clearance. Surface-bucket samples are sub-sampled by immersion of V4. Syringes are rinsed with sample water three times, including at least one bubble-free flushing, before the final drawing. Samples and syringe/valves are held under UV-free low light and analyzed as soon as possible, usually in less than 0.5 h of collection; 12-bottle CTD casts with duplicate samples require up to 2.5 h.

Samples from small-necked containers (200-ml BOD bottles; 100–1000-ml 24/40-necked quartz flasks for microbial and photochemical incubation studies) are drawn using ~10–25-cm-long, 1/8-in. o.d. dip tube (Teflon or PEEK (preferred)) that is force-fitted inside the male Luer of V4. A drain tube on the opposing valve port facilitates fill/flush cycles without breaking the siphon or introducing air. Samples of 120–130 ml drawn into (nominally) 100-ml glass syringes were found best for biological incubations. By coupling their valves to the 50-ml syringe's valve, they can be sub-sampled into 50-ml syringes. The latter are preflushed with low-CO water if the sample's [CO] is unknown or expected to be $<0.5$ nM. Before sub-sampling, ~0.2 ml of water was expelled from the incubation syringe to minimize potential CO contamination from the valve. Three $>34$-ml samples are obtained using ~7-ml rinses per sub-sample.

### 2.2. Analysis

The analytical setup is shown schematically in Fig. 1A–D. It consists of an RGA3 reduction gas analyzer

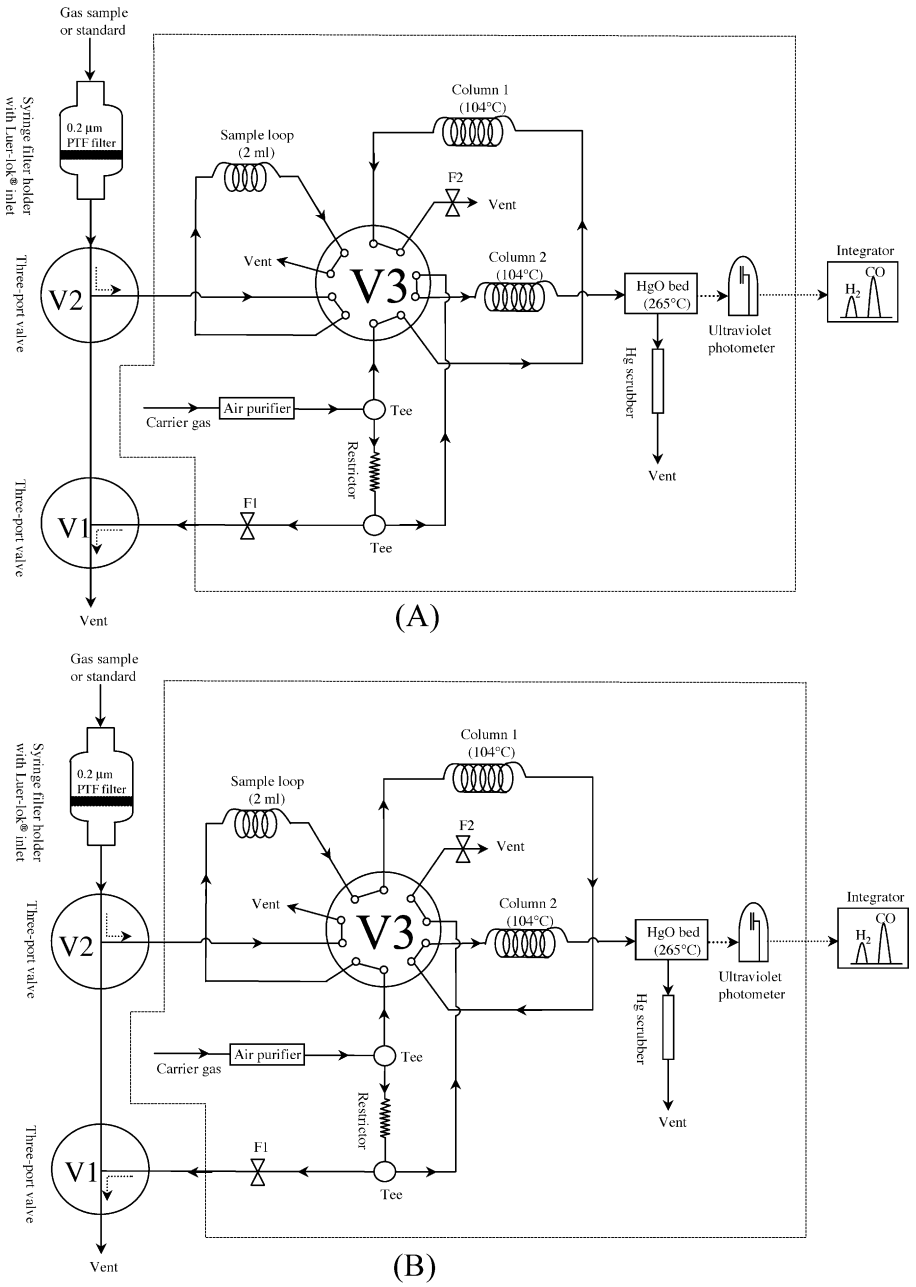


Fig. 1. Panels A and B: Reconfigured RGA-3 plumbing. The carrier gas is zero-grade CO-free air (Praxair or equivalent), optionally regulated by a mass flow controller. V1 is three-way ball valve (Whitey), V2 is a miniature three-port valve (Hamilton); V3 the RGA-3's 10-port sampling valve with a 2-ml stainless steel sample loop (Valco). Panel A: V3 in sample injection position (see also panel D); Panel B: V3 in sample chromatography position. After CO elutes, CO-free gas via V1 and V2 is used to provide headspace for another sample (panel C). The first column is packed with Unibeads 1S (60/80 mesh), and the second one with Mole Sieve 5A (60/80 mesh). Both columns are 0.32-cm wide and 76.8-cm long. The dashed line frames the original RGA-3 plumbing. Panels C and D: Sample preparation and injection device. Panel C: Headspace preparation. Before introduction of CO-free air into the syringe, excess water is expelled via V4 (dashed arrow); Panel D: Injection of equilibrated headspace gas into the RGA-3's sampling loop (see also Panel A). Solid arrows show directions of CO-free air and of wedge movement.

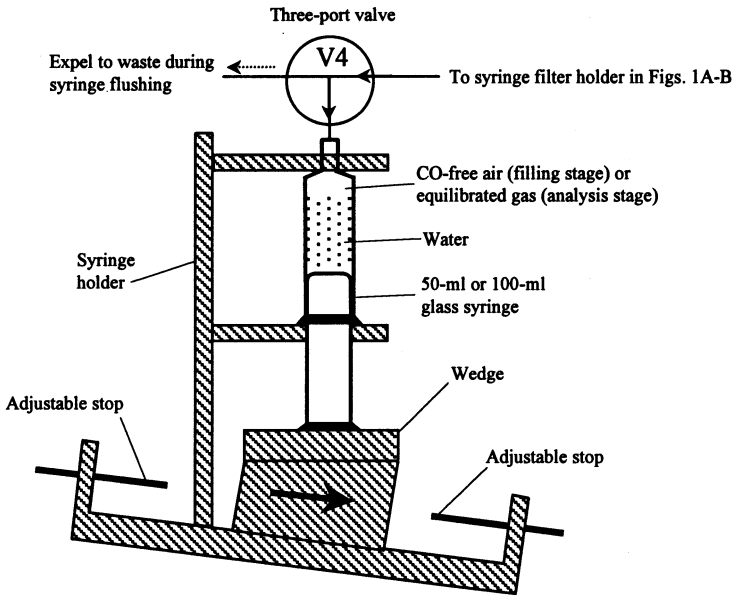


(C)

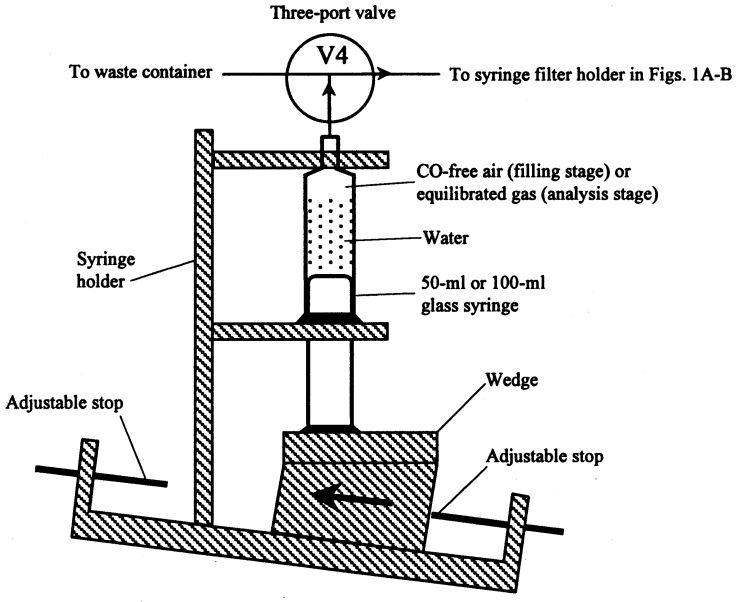


(D)

Fig. 1 (*continued*).

(RGD2 detector in a RGA3 chromatographic module, Trace Analytical, Menlo Park, CA) with an HP3396A (“HP”) integrator (Hewlett-Packard, Avondale, PA) or Chromatopac C-R6A integrator (Shimadzu, Kyoto, Japan). The RGA3’s plumbing was modified (Fig. 1A,B) and it was fitted with an adjustable syringe-holding device with a movable wedge (Fig. 1C,D) facilitating sample preparation and headspace gas injection. This device is used to obtain a precisely known sample volume by expelling excess water from syringes, to add a precisely known volume of CO-free headspace air (generated by a built-in air-purifier in the RGA3) at atmospheric pressure, and to inject the equilibrated headspace gas. The metal syringe filter holder containing a water-impermeable 0.2-μm Nuclepore Teflon filter (13-mm diameter) allows the sample loop to be flushed with headspace samples while reliably preventing any accidental, potentially disastrous introduction of liquid water (no water in over 10,000 injections). Air samples and gaseous standards are introduced without delay using water-wet 5-ml glass syringes with three-way plastic Luer® valves (V4).

If sample temperatures differ appreciably from room temperature, syringes are briefly immersed in room-temperature water before equilibration. These samples were randomly checked to ensure that their temperatures reach within 0.5 °C of room temperature before headspace preparation. The phases in 50-ml syringes are then equilibrated at room temperature and atmospheric pressure by vigorous agitation for at least 2 min with a Wrist-action® shaker (Burrell), or a vortex mixer (Glas-Col). A paint shaker (Hero Industries) is required for 100-ml syringes. Caution must be taken to clamp syringes without altering their internal pressures during equilibration. The syringes are placed in the holder (Fig. 1C), V4 is adjusted to waste, any water ($<0.2$ ml) usually in the syringe tip is expelled, V4 is set to inject, and almost all the equilibrated headspace gas is flushed through the filter and sample loop by sliding the wedge. The filter holder is dried and the filter is changed when blockage is detected as excessive backpressure. It is crucial to take great care that the inlet plumbing is leak-tight even under partial filter blockage due to wetting, which is easily tested by pressurizing for a few seconds with an air-filled water-wet 5-ml syringe.

Gas samples are injected onto a pair of chromatographic columns at $\sim 105$ °C to separate CO from hydrogen, the only other species detected in almost all seawater samples. The RGA-3 is delivered with backflushing of the first column to minimize the effects of any slow-eluting organic contaminants on the baseline; in our application, this flushing that starts 30 s after sample injection also permits the repeated injection of humid samples without degrading the system’s performance. Switching of V4 and starting the integrator are controlled by a home-built electronic timing device. After CO and hydrogen elute from the second column, they are carried to a hot HgO bed ($\sim 265$ °C), where they reduce mercuric oxide to mercury vapor which is quantified by an ultraviolet photometer. The resultant signals are recorded and integrated. At a carrier gas flow rate of $\sim 20$ ml/min, hydrogen (which is ubiquitous in air and often detectable in seawater) elutes at $\sim 0.33$ min and CO at $\sim 1$ min. A run time of 3–4 min adequately maintains a good baseline even after hours of sequentially injecting 100% humidity samples; presumably, water vapor is trapped on the first column and backflushed.

### 2.3. Calibration

The system is standardized every few hours, or before and after related sample blocks, by replicate injections of a commercial CO gas standard (e.g. nominal concentration: 1.14 ppmv in zero-grade air, analytical accuracy: $\pm 5\%$, Praxair, Bethlehem, PA). Multiple-point calibration curves are occasionally constructed to check the linearity of the system using volumetric (syringe) dilutions of the 1.14 ppmv standard or of a nominal 9.755 ppmv gas standard (Scott Specialty Gases, South Plainfield, NJ) with CO-free air (prepared by passing zero-grade air through a Trace Analytical CO scrubber). These curves are always linear below 2 ppmv CO with essentially zero intercept, and tests with CO-free air show that the injection process has an undetectable blank. For large data sets, it is convenient to correct data by interpolating standard peak areas over time periods between calibrations, after normalizing all values to area per unit retention time, since carrier-flow fluctuations cause most systematic calibration drift unless a mass flow controller is used (Fig. 1).

### 2.4. Calculation of CO concentration

The measured concentration of CO in the equilibrated headspace ($m_a$ in ppmv) is used to calculate the dissolved CO concentration ($\{CO\}_w$ in ml CO/ml $H_2O$) remaining in the water after equilibration:

$$\{CO\}_w = 10^{-6}\beta m_a p$$

where $\beta$ (ml CO/ml $H_2O$/atm) is the Bunsen solubility coefficient of CO, which varies as a function of temperature and salinity (Wiesenburg and Guinasso, 1979), and $p$ is atmospheric pressure (atm) of dry air. One unit of salinity variation causes less than 0.2% change in CO concentration. The presence of water vapor has no effect, because both the headspace samples and standards are saturated with water vapor, and are run at similar temperatures.

CO concentration in the initial seawater ($\{CO\}_{aq}$ in ml CO/ml $H_2O$) is calculated, assuming mass balance:

$$\{CO\}_{aq} = (\{CO\}_w V_w + 10^{-6} m_a V_a)/V_w$$
$$= 10^{-6} m_a(\beta p V_w + V_a)/V_w$$

where $V_w$ is the water sample size (ml), and $V_a$ is the volume of headspace air (ml). Conversion of $\{CO\}_{aq}$ to units in nM ($[CO]_{aq}$) gives:

$$[CO]_{aq} = 10^9 \times p\{CO\}_{aq}/(RT)$$

where $R$ is the gas constant (0.08206 atm l $mol^{-1}$ $K^{-1}$), and $T$ is temperature (K). In general, samples are equilibrated and analyzed within 1 °C of room temperature; if necessary (e.g. deep-water CTD casts), syringes are held in a bath at room temperature before analysis. It is estimated that 1 °C of uncertainty in temperature results in $<1\%$ uncertainty in CO concentration.

## 3. Results

Major aspects of the method and this section are summarized in Table 1 for casual readers.

### 3.1. Parameter optimization

Headspace/water equilibrium of CO in syringes is achieved after 1 min of vortexing or 2 min of agitation by the wrist-action shaker (50-ml syringes), and after 3 min of shaking (100-ml syringes); 3 or 4 min, respectively, are used, corresponding to the analytical run time. To use the system efficiently, gas extraction of the next sample is underway while the previous sample is under chromatographic separation and reduction detection (3 min); a third sample's headspace is loaded after the CO peak has integrated. This cycle leads to an analysis rate of up to 12/h. While 3 ml of headspace gas adequately flushes the sample loop (2 ml), nearly 5 ml is usually introduced.

The sensitivity and precision of this method depends on the water/gas volume ratio, $V_w/V_{air}$, which is easily and reproducibly adjusted using the stops for the movable wedge (Fig. 1C,D). At a given $V_w/V_{air}$, increasing the size of the sample loop increases sensitivity, but requires more gas to flush the loop, decreasing the water/gas ratio and hence the sensitivity. The volumes of the sampling loop (2 ml), the syringes (50 or 100 ml), and $V_w/V_{air}$ (7 or 18) chosen were found to be a good compromise for measuring CO in the open ocean ( $\sim$ 0–4 nM [CO]). For higher sensitivity, more awkward, expensive, delicate 100-ml glass syringes (90 ml water, 5 ml gas) were used in recent studies in the Sargasso Sea (R/V Endeavor-327 and 335), raising [CO] by a factor of $\sim$ 2.4 relative to the 7:1 ratio. The percentage of CO initially present that is extracted into headspace is 88% at 7:1 and 74% at 18:1. Theoretically, using a $p$CO equilibrator (e.g. $V_w/V_{air}>1000$, extraction approaching 100%) can yield headspace samples with $\sim$ 5 times higher [CO] and so is much better for low-[CO] samples, which approach the limits of the system. However, bringing the phases into contact and recovering gas for analysis at very high ratios poses formidable practical challenges.

### 3.2. Blanks

Instrumental noise and internal blanks of the RGA3 are negligible compared with sampling blanks associated with CO contamination from the samplers, the sub-samplers (syringes, plastic valves, V4, and possibly the cement attaching metal tips to glass syringes (50 ml only)). The sub-sampling process may also have a blank. Short-term syringe blanks were determined by repeatedly extracting the same water until the resultant CO signal reached a relatively

Table 1
Summary of CO sampling and headspace analysis methods optimized for marine studies (low CO concentrations)

| Process | Description/Parameters |
|---|---|
| In situ sampling | Use nonplastic samplers (Ti bottles, or stainless-steel pumping systems lines, or buckets (lowered sideways, calm to moderate conditions), or glass syringe samplers (Donoghue et al., 1998)). Cole-Parmer Bev-a-line P-06491-56 tubing may also be acceptable for short contact time with sample. Variable, frequent contamination of ~0–0.2 nM [CO] from PVC bottles (''Niskin'', ''Go-Flo'') is not traceable to specific ''bad'' bottles. Release of CO during/after photolysis of plastics is one cause. CO contamination has also been traced to or suspected from (1) diffusion of CO from motor brushes in enclosed housing through nearby Si tubing, (2) graphite-like grease packing in a Teflon-stainless steel valve, and (3) slowly leached contaminants (cutting oils, welding residues?) present in new Ti bottles. |
| Sub-sampling | Glass syringes (50- or 100-ml) with three-way Luer® plastic valves. Avoiding daylight, draw duplicates (three flushes). Avoid bubbles and stack gases; keep valves in dim light or dark at all times. Avoid dirtying exposed barrel surfaces to maintain easy motion. |
| Sample storage | Minimize storage time/light exposure. Bring samples to room temperature ±1 °C. Typical storage: 2–10 min for one bottle with duplicates; 1–150 min for a 12-bottle CTD cast (not recommended for low [CO]). |
| Equilibration | Wedge device used to set precise volumes of headspace air (CO-free air supplied by the RGA3) and water. Typical water/air ratios are 7:1 (50-ml syringes); 18:1 (100-ml syringes). Equilibration by ~3 min (50-ml syringe) or ~4 min (100-ml syringes) of vigorous shaking. Clamp syringes, avoiding alteration of syringe's internal pressure while equilibrating. |
| Analysis | 5 ml of wet air directly injected (2-ml loop) through 0.2-μm Teflon hydrophobic filter. No effect of water vapor (>$10^4$ runs on one column pair); 3-min isothermal (104 °C) separation on two columns (first column backflushed after 30 s). Carrier gas (zero grade air) flow rate: ~20 ml/min. Detection by HgO reduction (265 °C). Peaks integrated by Shimadzu integrator. |
| Standards | Routine single point calibration by moist ~1-ppmv CO standard in air. Occasional internal blanks and linearity checks by syringe dilution of 1-ppmv standard. Sample CO-free water and aqueous CO standards for highest confidence. |
| Calculation | Normalize peak areas to standard gas by interpolation. Correct for unextracted CO using solubility data. |
| Performance | 8–12 samples (with standards)/h. Syringe blank: <0.03 ± 0.004 nM. Precision: better than ±0.018 nM ± 2% at typical surface concentrations; better than ±0.004 nM ± 13% at syringe blank levels. Variability in duplicate measurements: 0.035 nM (4.5%). Accuracy: better than ±10%. Linear range: ~0–12 nM. Carrier flow: mass flow controller recommended. |
| Miscellaneous | Draw coastal and lowest-level samples in darkness (flashlight) due to extreme sensitivity to light. Check for and remove water in filter holder; if needed, replace filter and pressure-leak-test. Extremely high concentrations of $H_2$ (due to corrosion) can interfere with CO peak integration. Analyze over-range samples by lowering water/gas ratio, using smaller sampling loop, dilution with low-CO water, or by repeatedly extracting samples. System/procedure is very motion-insensitive (some S/N increase in rough weather). See also inter-calibrated automated version (Xie et al., 2001). |

constant value. Fig. 2 shows a 1999 test of 50-ml syringes with new Kontes valves kept away from sunlight. CO signals were recorded by both HP and Shimadzu integrators, using integration parameters selected with the intent of optimizing quantification. The integrators agreed well at high CO concentrations, but at low CO concentrations, data from the HP integrator were more scattered than those from the Shimadzu. The HP integrator sometimes does not detect small peaks that were resolved and quantified by the Shimadzu integrator (e.g. point #6 in Fig. 2). Important undetected HP peaks were recovered approximately by a peak height vs. peak area regression derived using small peaks that were detected. Time-dependent blanks were determined by extracting to near-zero signal, adding headspace, and remeasuring after variable delays (Fig. 3).

The syringe/sampling blanks from a variety of tests are summarized in Table 2. These blanks in principle include any CO production by water samples, but their similarity (using different waters and water volumes) suggests that these signals are primarily method/syringe blanks. Blanks for samples analyzed soon after collection are likely small and reproducibly in the range 0.02–0.04 nM, but blanks may increase significantly and less reproducibly after 0.5–1 h. Efforts to find affordable, reliably blank-free alternative gear have failed.

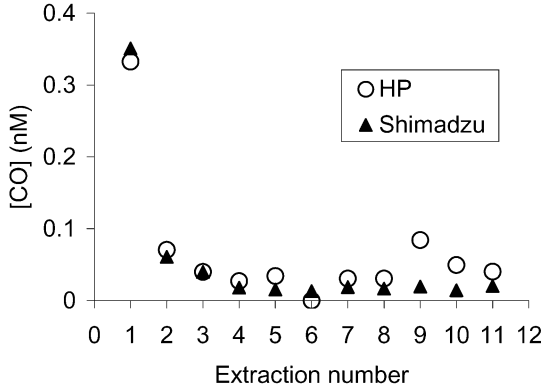


Fig. 2. Low-level [CO]: tests of syringe (50 ml) blanks and integrators by repetitive extraction (at ~5-min intervals) and analysis of a water sample collected from Vineyard Sound, Woods Hole, Massachusetts. HP stands for the HP3396A integrator, and Shimadzu for the Chromatopac C-R6A integrator, both with parameters optimized. Extraction #6 was not detected by the HP integrator.

### 3.3. Linearity, precision, and accuracy

Fig. 4 shows a typical multiple-point calibration curve constructed by volumetric dilutions of the 9.755 ppmv gas standard with CO-free air. The analytical system responded linearly up to at least 1.86 ppmv CO, corresponding to 11.8 nM for 50-ml syringes or 5.5 nM for the 100-ml syringe at 1 atm, 25 °C, and salinity 36. CO concentrations in marine waters are usually far below these values, but in coastal regions, concentrations above 20 nM have been observed (Ohta et al., 2000). Over-range samples can be analyzed by lowering the water/gas ratio, by using smaller sampling loops, or by dilution with low-CO water in extreme cases. Samples can also be reanalyzed by reequilibration with fresh headspace gas and an initial [CO] value calculated with slight loss in accuracy. The analytical precision was also evaluated in these tests. The concentration of the aqueous standard prepared from the 1.23-ppmv gaseous standard is approximately typical of average CO levels in marine surface waters (Bates et al., 1995). Table 2 shows that the reproducibility at the 1.23-ppmv level was better than ± 0.022 ppmv ± 2% (or ± 0.018 nM ± 2%). At the trace levels of the syringe blanks, the reproducibility was better than ± 0.004 nM ± 13% (see Section 3.2 and Table 2).

Accuracy seems to be affected primarily by uncertainties in gas standards, which may be time-dependent (Novelli et al., 1991). At 1-ppmv levels, inconsistencies of up to 30% have been noted among certified tanks (Novelli et al., 1991 and references therein). After 2 years, the nominal 1.14-ppmv tank used for standardizing our system was calibrated recently against a newly purchased 9.755 ppmv tank traceable to the NIST (the US National Institute of Standards and Technology) reference scale. The recalibrated concentration was found to be 1.23 ppmv, 8% above the supplier's certified concentration. The manufacturer's analytical errors can account for up to 6% of this difference. The analytical uncertainty due to using the 1.14-ppmv standard during the past 2 years should be better than 15% based on the NIST recalibration; changes are negligible over the time scale of months and field studies.

The accuracy was also evaluated by measuring the recovery of aqueous CO standards prepared by continuously bubbling ~ 600 ml of aged seawater with certified gaseous standards (expected to reflect equilibrium values to better than ± 1%). The aqueous standards were then analyzed as ordinary water samples. The results are shown in Table 3. The ratios, though showing some scatter, average 97% for all conditions. The scatter suggests that our results are generally accurate

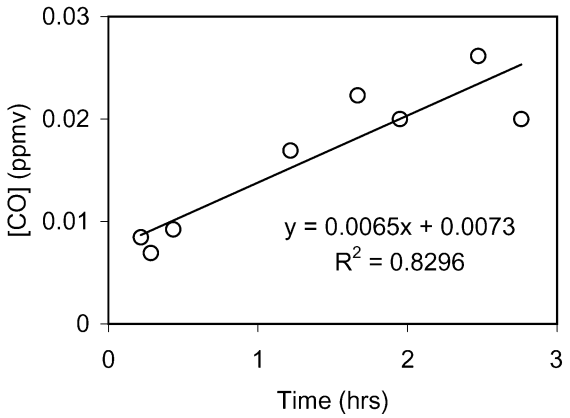


Fig. 3. Time-dependent syringe blank regression from *Weatherbird* 97 study. The regression, converted to [CO] is presented in Table 2. These values depended little on the volume of water in the syringe; they are total blanks, thought to be mostly or entirely syringe/valve-derived.

Table 2
CO blank results for syringe/valve/sampling process

| Syringe/valve | Inferred blank (nM [CO]) | Extraction method | Remarks |
|---|---|---|---|
| 50 ml not Kontes | 0.07 | Multiple sequential | $n=1$, 5-min intervals. *Oceanus*-256. Valve's sunlight exposure history is unknown. HP. |
| 50 ml Kontes | $0.02 \pm 0.002$ | Sequential extraction | $n=8$. Five min intervals. (Fig. 2). Randomly chosen valve from *Endeavor*-335. Shimadzu. |
| 100 ml (all-glass) Kontes | $0.03 \pm 0.004$ | Sample/analyze "zero CO" water | $n=7$. Randomly chosen valves from *Endeavor*-335, no time delay. Process includes the fill-flush-sample process. Zero water was old open-ocean seawater extensively bubbled with CO-free air. Shimadzu. |
| 50 ml Kontes | $0.05+0.043^{*}$(h); $n=8$, $r^2=0.82$ | Reextract near-zero [CO] water after 0–2.5-h delays | h = hours in syringe. Eight syringe/valve pairs (R/V *Weatherbird* 08/96). Results depended little on water volume ( ~ 5 to ~ 30 ml). HP, small peaks by peak height. See Fig. 3. |
| 5 ml (all-glass) Kontes | 0.007 nM/h (50-ml syringe) 0.003 nM/h (100-ml all-glass syringe) | Sequential extraction | Water-moistened syringe, various time delays, valves randomly chosen from set used on *Endeavor*-335. Five pmol/h CO flux assumed due to plastic valve. Shimadzu. |

to $\pm$ 10%. The system's accuracy and precision are also affected by fluctuations in the carrier-gas flow, which can be large and change rapidly when the carrier gas regulator is outdoors, exposed to wind and sun. Changes in flow, indicated by shifts in the peaks' retention time, change the residence time of mercury vapor in the detector and hence CO peak areas. This effect can be minimized by frequent injection of CO standards and by normalizing peak areas to retention times, or eliminated by using a mass flow controller.

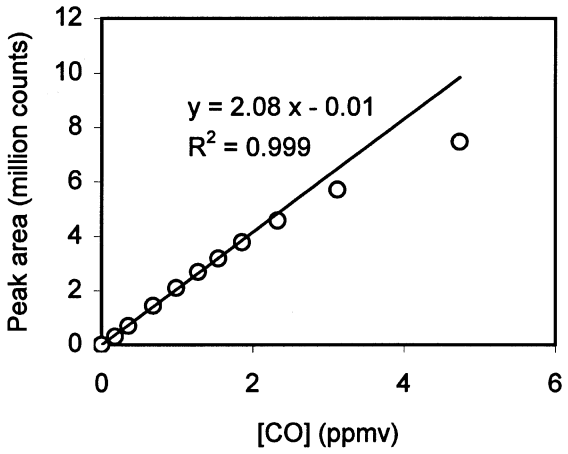


Fig. 4. Typical calibration curve constructed by volumetric dilutions of a 9.755 ppmv CO standard with CO-free air. Each data point represents the mean of triplicate analyses. Also shown is the linear regression curve for the first eight data points. Peak areas were recorded with a Shimadzu Chromatopac C-R6A integrator.

### 3.4. CO sampling and contamination

Methods for natural water analysis are nearly useless without adequate samplers. The large diurnal variability of [CO] and a factor of two uncertainties in gas exchange coefficients (Bates et al., 1995) has permitted aspects of CO cycling to be explored productively with methods of little-described precision and accuracy. However, better data, especially data suitable for modeling studies, will require well characterized measurements of high quality to distinguish true model–observation discrepancies from measurement uncertainties. These issues prompt us to report at length below on CO sampler issues in the same paper reporting our method and its validation.

#### 3.4.1. Potential for sampler contamination artifacts

Experience on ~ 10 process-oriented cruises slowly suggested that CO contamination at levels $<0.3$ nM is likely an erratic but endemic problem with Niskin and Go-Flo samplers. Such CO levels are common near dawn and below the mixed layer (ML).

Table 3
Recovery of aqueous CO standards prepared from gaseous CO standards

| Syringe size (ml) | Water/gas ratio | Gas standard (ppmv) | Aqueous standard, measured (ppmv) | | | Ratio of aqueous vs. gas (%) |
|---|---|---|---|---|---|---|
| | | | Mean | $\sigma$ | n | |
| 50 | 7 | 1.23 | 1.08 | 0.015 | 6 | 88 |
| 50 | 7 | 4.99 | 5.18 | 0.055 | 6 | 104 |
| 50 | 7 | 9.77 | 10.56 | 0.22 | 5 | 108 |
| Mean (50) | | | | 0.08 | | 100 |
| 100 | 18 | 1.23 | 1.16 | 0.022 | 5 | 94 |
| 100 | 18 | 4.99 | 4.48 | 0.075 | 5 | 90 |
| Mean (100) | | | | 0.048 | | 92 |

Attempts to identify individual "bad" samplers or to measure bottle-specific blanks failed. As tracking down erratic contamination involves detecting small [CO], rapid progress was made only after beginning frequent inlet system leak tests, using peak heights to recover undetected small signals (or using Shimadzu integrators), and identifying the confounding influence of time-dependent sub-sampling syringe blanks (Table 2, 4th data row). Our cumulative experiences and some initial experiments led to several ideas about the sources and behavior of CO contamination associated with plastic bottles.

- Mixing in a full water-filled bottle is extremely slow without external agitation with an air bubble or added objects (marbles), so contamination emitted by sampler surfaces may mix erratically into sub-sampled water.
- Incubating parts of a used 5-l General Oceanics Niskin under poisoned low-CO seawater in a sealed glass chamber under dim room light overnight showed CO production; incubated separately (most in water-wet syringes), *all* components (gray PVC end cap, Delrin® valve, gray plastic-coated spring, Nylon® line loops, and red Silicon rubber O-rings) generated CO.
- The rates of CO formation from these components were clearly significant but difficult to relate to a whole bottle. Delrin® was by far the most prolific per unit area; but the PVC endcap flux indicated that PVC would dominate the total flux due to its much larger area.
- "Soaking" bottle components in nitrogen or washing them with acid or freshwater did not dramatically change CO formation rates, suggesting that microbial production and outgassing of contaminant CO were not likely to be sources.
- The sub-sampling valve attached to the bottle traps water in a small annulus surrounded by Delrin, PVC, and Si O-rings. This water enters the sample when the valve is opened, possibly allowing large, variable [CO] to build up and to be erratically sub-sampled.
- Air samples from ship and land labs, and at CTDs during sampling, usually showed [CO] $<250$ ppbv, so ingress/dissolution of contaminated air is not likely the major cause of contamination.

### 3.4.2. CO sampler contamination tests at sea

Two ensuing experiment series, to be detailed in a paper on our Titanium sampler (in preparation), verified the existence of difficulties with Niskin samplers, though not settling all issues. On CALCOFI 9704 (*New Horizon*), we tested SIO's Niskin-style bottles that had white PVC bodies, flat gray PVC end caps, khaki-colored Viton® O-rings, and metal springs. Filled with water from 150 to 550 m, they generated CO internally at $\sim 0.3$ nM/h. This CO could (implausibly) be associated with a process initiated somehow in the water by the sampling and/or retrieval process, especially as these samples were sub-oxic; however, it seemed most likely to be contamination.

We then devoted a 1-week *Weatherbird* cruise in August 1997 to intensive sampler testing, emphasizing deep water (mainly 100–1000 m) where [CO] is expected to be low and reproducible in replicate casts. Samplers included $\sim 8$ of BBSR's standard 12-l General Oceanics Niskins in use daily by the BATS team, six randomly selected General Oceanics 10-l Niskins (WHOI CTD group), shipped to Bermuda, and kept aboard in darkness during the day, and a glass syringe sampling device designed for $SF_6$ tracer work (Donoghue et al., 1998). All work was done at night to minimize light effects on samplers (see

Section 3.4.3) and samples (deep waters being more light-sensitive; Kieber et al., 1989). Samplers were tripped on down- and up-casts, giving samples from each depth with known, markedly different times in samplers. This large workload resulted, for the first time, in large numbers of low-[CO] samples awaiting analysis in sub-sampling syringes (not the in situ sampling syringes) for up to 2.5 h. The sub-sampling syringe blank itself was found to be time-dependent (Table 2, 4th data line). Correcting the primary sampler data for this effect as well as possible considerably increased the uncertainty in already-small signals. Principal results were: (a) samples in glass syringes gave the lowest, most reproducible values, ~ 0.07 nM [CO] from 100 to 4000 m (these results were not notably dependent on time-in-sampler); (b) on average, the Niskins gave more scattered and higher results (up to 0.2 nM, often ~ 0.1 nM); (c) [CO] in Niskins appeared to increase over time-in-Niskin; (d) initially, the WHOI Niskin values were highest, but they gradually approached the BBSR Niskin values over several days. These results further confirmed the contamination of CO by plastic samplers and its variability and dependence on the samplers' irradiation history.

### *3.4.3. CO photoproduction and post-irradiation emission from polymers*

Also on CALCOFI 9704, initially clean air-filled 1/4-in. PTFE tubing sitting < 1 h in late afternoon sun was found to contain very high-[CO] air. Subsequent experiments showed that CO was formed by sunlight (but not lab light) and continued to evolve afterwards for hours. The near-transparency of PTFE at solar wavelengths and its oxidation-defying structure suggested that other polymers might be even more reactive, and that post-irradiation CO emissions might be complex functions of polymer chemistry, light history, transparency, diffusion coefficients of $O_2$ and CO, temperature, etc. (presumably, light effects on prior tests were minimal due to night work on the Weatherbird).

In fact, studies of photoproduction of CO (and $CO_2$) from synthetic organic polymers can be traced back to early 1960s. Wilks (1963) observed evolution of CO from Tygon, polyethylene, Lucite, natural rubber, and Teflon when these materials were exposed to natural solar radiation in the presence of oxygen. Siegel and Hedgpeth (1967) explored the mechanism of CO production by Teflon under $\gamma$-radiation. Using a sunlight exposure chamber continuously flushed with CO-free air (Fig. 5), we tested CO production by PVC, PTFE, silicone rubber, Buna-n rubber, and other samples that are widely used for CO sampling and analysis. After flushing out background air, the flask was either exposed to natural sunlight or darkened with aluminum foil. Fig. 6 (top) illustrates the results of tests on Teflon (spring-time cloud-free conditions) and PVC (variable clouds). The CO levels rose rapidly to about two and six times clean-air [CO], despite continuous flushing with clean gas. After darkening the samples, CO concentrations decreased rapidly because of dilution by the CO-free flow, but leveled off at above-blank values. To confirm that CO continued to be emitted after switching from light to dark, we injected a small amount of $H_2$ as an inert dilution tracer into the flask immediately before darkening it and monitored the $H_2$/CO peak area ratio. This ratio would remain constant if [CO], like [$H_2$], were controlled only by dilution by CO- and $H_2$-free inflow. Fig. 6 (bottom) shows that the $H_2$/CO ratio decreased with time, clearly indicating continued emission of CO over time scales of tens of minutes. The emission

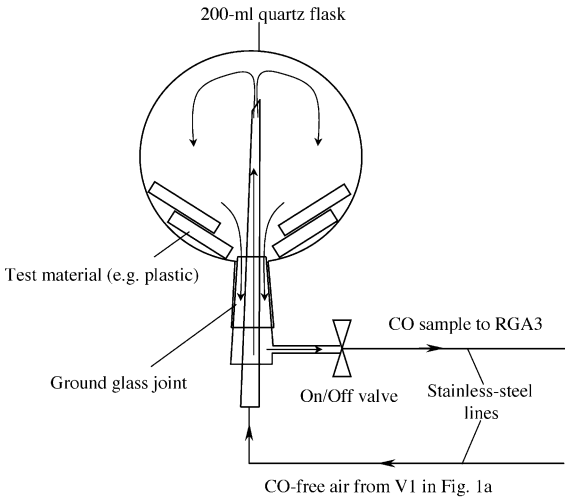


Fig. 5. Sunlight exposure device for CO contamination tests. The quartz flask was either exposed to sunlight or covered with aluminum foil. The valve was light-shielded to keep the background low. Flushing gas from V1 ( ~ 20 ml/min, 1/*e* flushing time ~ 10 min) was returned to the RGA3 for quantification.

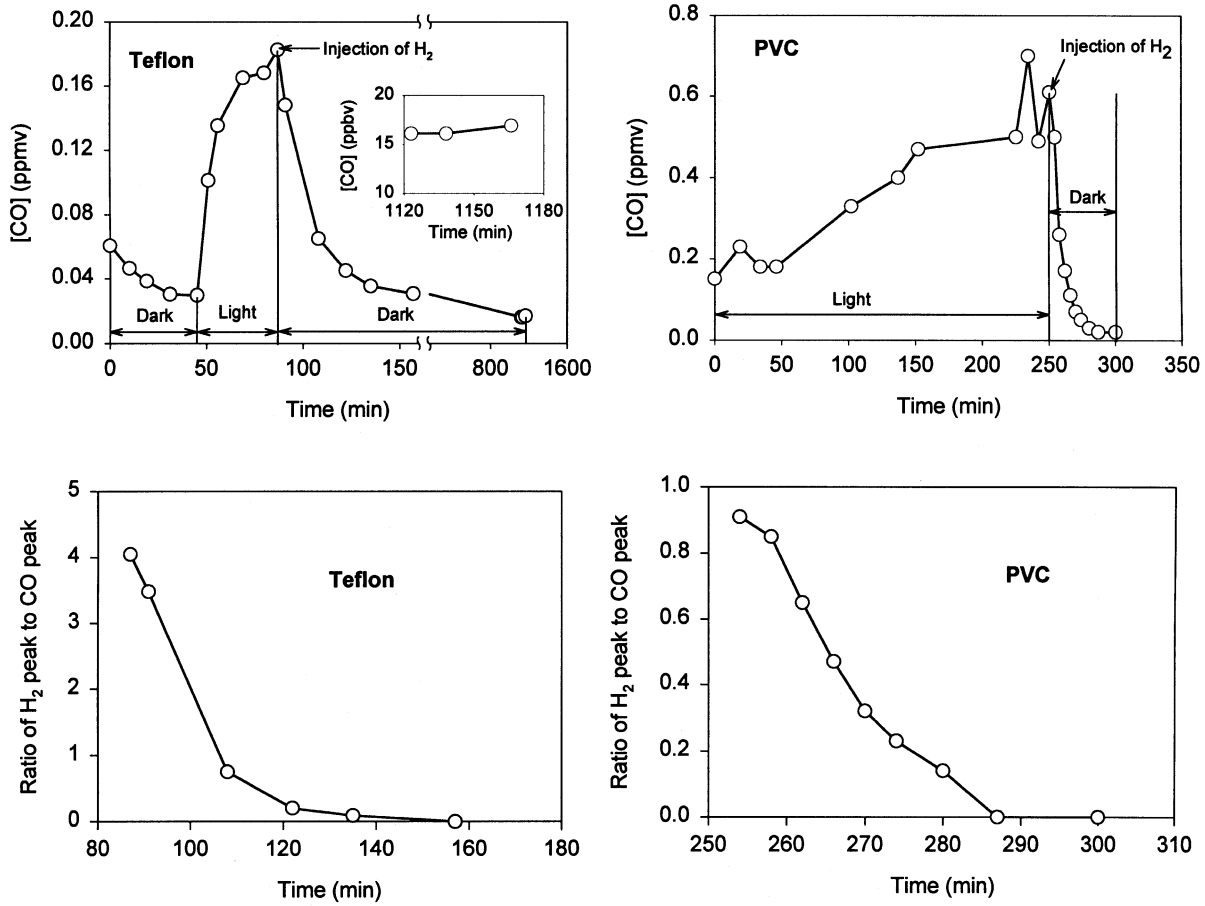


Fig. 6. Upper panels: CO production by plastics (Teflon and PVC) as a function of time under light and dark conditions. Hydrogen spike is used as a dilution tracer. Lower panels: The $H_2$/CO peak area ratio as a function of time after the irradiated plastics were darkened. In the Teflon test, the flask had been exposed to sunlight briefly before $t=0$. Declining ratios indicate that CO is being evolved continually.

involves some combination of post-irradiation production and diffusion of CO. Other polymers tested all generated CO during and well after light exposure; their photoproduction rates were all much higher than the dark production rates. (Solar heating, may be a factor in the CO emission rates, especially of dark-colored materials.) Wilks (1963) did not observed dark production of CO from the polymers he tested probably due to the relatively low sensitivity of his method. Our tests qualitatively indicate that Buna-n rubber and Teflon are less CO-contaminating than is silicone rubber, which in turn is better than PVC. Later, at-sea tests showed that Bev-a-line tubing (Cole-Parmer catalog # P-06491-56) is useable for CO in sunlight for short-time contact with seawater.

To summarize sampling issues, plastic samplers ("Niskins", "Go-Flos", etc.) are likely to contaminate high-precision CO samples at erratic, sampler-history-dependent rates. We believe that such samplers routinely contaminate at *roughly* the ~ 0.05–0.25 nM [CO] level; a PVC sampler tripped in clear water close to the surface in full sun might well show greater effects that seem almost impossible to quantify. Clearly, such light-dependent artifacts would be especially damaging to studies of CO photochemical cycling in the mixed layer. While good low-level deep-water CO samples from some PVC samplers may be obtainable, major efforts would be required to validate them. The quality of published [CO] data from bottles thus seems very unclear, although fortunately, many

published [CO] data are from underway surface-sampling systems.

## 4. Applications

### 4.1. In situ samples: validation of sampling methods

The system and new sampling methods were used on R/V *Endeavor* cruises in the Sargasso Sea in August 1999 and March 2000 for measuring in detail the diurnal upper-ocean CO cycle — distribution and photoproduction (Xie et al., 2000; Najjar et al., 2000; Zafiriou et al., in preparation). An all-inclusive estimate of analytical variability for in situ samples obtained using nonplastic samplers was estimated based on measurements of 130 duplicates from a Titanium bottle by three analysts during a cruise in the Sargasso Sea in August 1999 (R/V *Endeavor*-327). The average CO concentration was 0.78 nM (range: 0.02–2.38 nM); the average difference in each pair was 0.035 nM, or 4.5%. Sample quality was also established by comparing Ti bottle samples with two other methods: a stainless steel bucket lowered sideways with a trip-line (in low to moderate winds), and an automated stainless steel surface pumping system (in preparation). The 1-m titanium bottle samples agreed within 4.9% ($n=9$) with bucket samples and within 5.4% ($n=5$) with the 1-m pumping system. All three sampling methods thus appear to be valid within our current precision.

### 4.2. Vertical profile of [CO]

Fig. 7 shows a detailed vertical profile of [CO] down to 200 m (along with the density structure) obtained near the BATS site in August 1999 (R/V *Endeavor*-327) using the titanium sampler and the headspace system. Samples from 200 m were frequently collected during that cruise; the concentrations of these samples are all presented in Fig. 7. [CO] peaked at the surface and decreased rapidly through the top 100 m. The concentration at 200 m averaged 0.03 nM ($\sigma=0.01$, $n=11$), which was at the same level of the syringe blank (see Table 2, 3rd data row). This value is 3–30-fold lower than the open-ocean deep [CO] reported by other groups using Niskin bottles (Conrad et al., 1982; Jones, 1991; Johnson and Bates, 1996). Our profile, however, did indicate significant [CO] well below the seasonal ML, which was always less than 40-m thick and was underlain by a sharp pycnocline during the time of investigation (Fig. 7). As the 1% light level at the wavelength of peak CO photoproduction (320 nm; Kettle, 1994; Kettle et al., 1994) was only ~40-m deep, this observation suggested either nonphotochemical oceanic CO sources at depth (e.g. photobiological production) or substantial photochemical CO formation initiated by longer wavelengths that had deeper penetration depths.

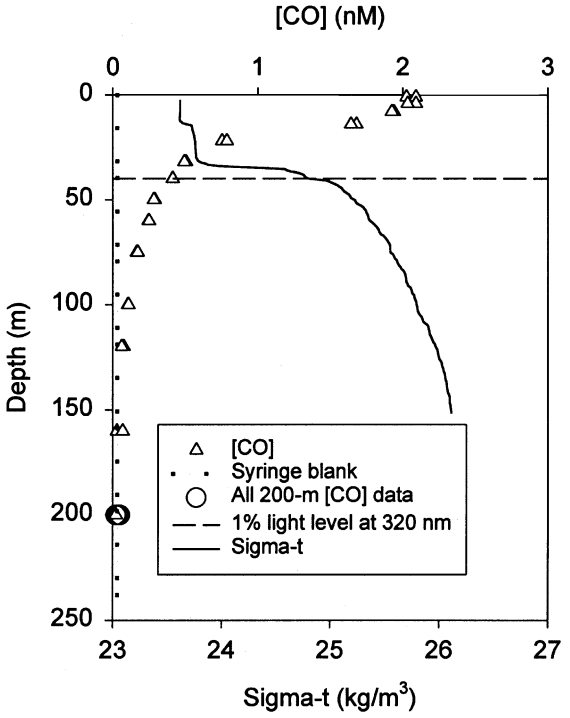


Fig. 7. Vertical profile of [CO] obtained at 31.52°N, 63.57°W in the Sargasso Sea in August 1999 using a titanium sampler and the headspace analysis system. Also shown is the corresponding density structure.

### 4.3. Incubations: biooxidation of CO

The system has also been used in process studies: photoproduction, both in situ and in laboratory irradiations; incubations of unfiltered seawater for measuring the (net) microbial loss rate of CO in the dark; and incubations aimed at detecting light-independent

(“dark”) chemical or biological CO production. Such applications are illustrated below for the most intensively used type of study, net biological decay rates.

CO is known to be consumed microbially in natural waters (Conrad et al., 1982; Jones, 1991; Johnson and Bates, 1996; Ohta et al., 1999; Zafiriou, unpublished data. In initial work during *Oceanus*-256 (Kettle et al., 1994) and RITS94 (R/V *Surveyor*), six or more aliquots per Niskin bottle were drawn into 300-ml glass BOD bottles as though they were dissolved oxygen samples (referred to as “BOD method”). The bottles were darkened with electric tape or aluminum foil, and incubated within 2 °C of sea surface temperature. BOD bottles were used only once each; samples for analysis were drawn at various times into 50-ml glass syringes and analyzed over up to 48 h. The data were plotted as a time series and fitted with an exponential decay curve. The BOD method required much water and tedious drawing, and gave rather scattered data, due mainly to high scatter in the initial [CO] of nominally identical BOD samples. Hence, in all subsequent cruises, we drew duplicate samples directly into acid-cleaned 100-ml all-glass syringes, incubated them in a cooler maintained at near sea-surface temperature, and analyzed the sequential sub-samples, usually at ~ 10-h intervals, as described above. The all-glass construction (with plastic valves) permitted acid cleaning and minimized the chances that metal contamination would affect the microbial community during incubations. The samples were usually taken in daytime well after dawn, so [CO] was higher than its local 24-h average, and decayed through a concentration range very roughly similar to that occurring in the water column over a daily cycle.

During the past several years, a large dataset of CO net first-order decay constants in marine waters has been generated using the syringe method. Fig. 8 shows two time-series dark incubations conducted aboard the R/V *Discoverer* during ACE-1 in the North and South Pacific in October/November 1994. The results in Fig. 8 are only intended to illustrate this dataset. Multiple data points for several syringes were combined to better define the curves, whereas usually only three time points are used to define a rate, the duplicate syringes being sampled in parallel and plotted separately to minimize the effect of any differences in initial [CO] ($t=0$). CO concentrations decreased exponentially with incubation time, and CO decay constants obtained by exponential regression were 0.70 and 0.79 day$^{-1}$ for the two examples. The data are quite consistent as indicated by the high $r^2$ values. The possibility of physical loss of CO through leaking out of the syringe tip was tested by adding CO in sterilized water and incubating it over time periods (up to 2 days) similar to the biooxidation incubations. We did not see any significant change or consistent trends in [CO] in the syringe. Although very low [CO] values might be significantly influenced by the syringe (valve) CO blank term, in practice, incubations rarely lasted long enough for samples to decay to very low levels, and any valve contaminants should not enter the syringe, since in 100-ml glass-tip syringes there is ~ 100 μl of water at the Luer tip insulated from the bulk sample by a cylindrical channel ~ 11-mm long and 1-mm in diameter that is flushed every sampling ( ~ 10 h). In the absence of convection, the diffusion time for contaminating CO to enter the sample via this channel is calculated to be ~ 5 days.

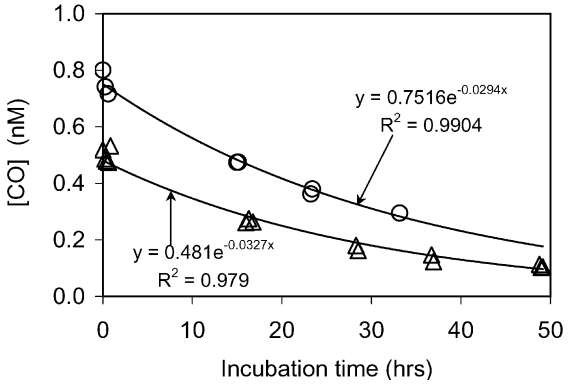


Fig. 8. Concentration of CO as a function of time during dark incubations using water samples from the Pacific in October/November 1994. Solid lines are the exponential fits of the data. The loss is microbially mediated, as shown by filtration and poisoning experiments.

## 5. Summary

A headspace analysis method with well demonstrated accuracy and precision was developed for

measuring trace levels of CO in natural waters and for process studies of the CO cycle. Alternative samplers were also found to be necessary for reliable low-level [CO] work. Table 1 gives an overview of the sampling and analysis approaches, which are efficient, simple, convenient, and robust enough to be used under inclement conditions. It provides an alternative approach to the traditional purge-and-trap technique. We have also designed, built and used an automated, continuous-flow equilibration CO analysis system intercalibrated with this method (Xie et al., 2001). The system and sampling methods were used on R/V *Endeavor* cruises in the Sargasso Sea in August 1999 and March 2000 for studying the diurnal upper-ocean CO cycle intensively (Xie et al., 2000; Najjar et al., 2000).

Evidence is presented to show that plastics and polymers, especially the traditional and nearly universal PVC samplers (Niskin and Goflo® bottles), may introduce substantial, erratic CO contamination at several different points in the analytical cycle, especially for low-CO (dawn, sub-ML) samples. For this reason, we believe that no accurate deep CO profiles have yet been documented, and that most ML data taken during the day may also contain artifacts of varying magnitude. We have no evidence that the photolysis of plastics is likely to influence any other commonly measured oceanographic variables, but oceanographers measuring trace organic substances might wish to rule out this possibility.

## Acknowledgements

We have learned much about CO analysis through discussions with J. Bullister, J. Johnson, R. Jones, and P. Novelli. We thank the captains and crews of R/V *Discoverer*, *New Horizon*, *Oceanus*, and *Weatherbird*; also, Chief Scientists Tim Bates, Tom Hayward, and Kjell Gundersen. The patient slaving of Jed Goldstone, Jason Schwaber, John Tolli, and Christopher Zafiriou during contamination identification and control cruises over the years was essential. We thank Mary Scranton for use of the RGA3 reduction gas analyzer, and Jim Ledwell and Terence Donoghue for loan and coaching in use of the glass syringe sampler. This work was funded by grants from ONR, NASA, and especially NSF OCE 9417214 and OCE 9811208. H. Xie acknowledges support from a WHOI Postdoctoral Fellowship. This is Contribution number 10501 of the Woods Hole Oceanographic Institution.

*Associate editor*: Dr. James Bauer.

## References

Bates, T.S., Kelly, K.C., Johnson, J.E., Gammon, R.H., 1995. Regional and seasonal variations in the flux of oceanic carbon monoxide to the atmosphere. J. Geophys. Res. 100 (D11), 23093–23101.

Bourbonniere, R.A., Miller, W.L., Zepp, R., 1997. Distribution, flux, and photochemical production of carbon monoxide in a boreal beaver impoundment. J. Geophys. Res. 102 (D24), 29321–29329.

Bullister, J.L., Guinasso Jr., N.L., Schink, D.R., 1982. Dissolved hydrogen, carbon monoxide, and methane at CEPEX site. J. Geophys. Res. 87 (C3), 2022–2034.

Conrad, R., Seiler, W., Bunse, G., Giehl, H., 1982. Carbon monoxide in seawater (Atlantic Ocean). J. Geophys. Res. 87 (C11), 8839–8852.

Derwent, R.G., 1995. Air chemistry and terrestrial gas emissions: a global perspective. Philos. Trans. R. Soc. London, Ser. A 351, 205–217.

Doney, S.C., Najjar, R.G., Stewart, S., 1995. Photochemistry, mixing and diurnal cycles in the upper ocean. J. Mar. Res. 53, 341–369.

Donoghue, T., Ledwell, J.R., Doherty, K., 1998. Water samplers for open ocean tracer release experiments. Technical Report, WHOI-98-20.

Gnanadesikan, A., 1996. Modeling the diurnal cycle of carbon monoxide: sensitivity to physics, chemistry, biology, and optics. J. Geophys. Res. 101 (C5), 12177–12191.

Johnson, J.E., Bates, T.S., 1996. Sources and sinks of carbon monoxide in the mixed layer of the tropical South Pacific Ocean. Global Biogeochem. Cycles 10 (2), 347–359.

Jones, R.D., 1991. Carbon monoxide and methane distribution and consumption in the photic zone of the Sargasso Sea. Deep-Sea Res. 38 (6), 625–635.

Kettle, A.J., 1994. A model of the temporal and spatial distribution of carbon monoxide in the mixed layer. MSc thesis, WHOI/MIT Joint Program, Woods Hole, MA, 146 pp.

Kettle, A.J., Martin, W.A., Zafiriou, O.C., 1994. Observations and numeric simulations of the diurnal flux of CO in the upper ocean. Trans. Am. Geophys. Union 75, 149.

Kieber, D.J, McDaniel, J.A., Mopper, K., 1989. Photochemical sources of biological substrates in seawater: implications for carbon cycling. Nature 341, 637–639.

Najjar, R.G., Erickson III, D.J, Madronich, S., 1995. Modeling the air-sea fluxes of gases formed from the decomposition of dissolved organic matter: carbonyl sulfide and carbon monoxide. In: Zepp, R.G., Sonntag, C. (Eds.), The Role of Non-Living Organic Matter in the Earth's Carbon Cycle. Wiley & Sons, New York, pp. 107–132.

Najjar, R.G., Werner, J., Zafiriou, O.C., Xie, H., Wang, W., Taylor, C.D., 2000. A one-dimensional model of carbon monoxide in Sargasso Sea surface waters (Talk OS21K-05). Trans. Am. Geophys. Union 80 (49), 93.

Novelli, P.C., Elkins, J.W., Steele, L.P., 1991. The development and evaluation of a gravimetric reference scale for measurements of atmospheric carbon monoxide. J. Geophys. Res. 96 (D7), 13109–13121.

Ohta, K., 1997. Diurnal variation of carbon monoxide concentration in the Equatorial Pacific upwelling region. J. Oceanogr. 53, 173–178.

Ohta, K., Inomata, Y., Sano, A., Sugimura, K., 2000. Photochemical degradation of dissolved organic carbon to carbon monoxide in coastal seawater. In: Handa, N., Tanoue, E., Hama, T. (Eds.), Dynamics and Characterization of Marine Organic Matter. Terrapub/Kluwer. Academic Publishers, Tokyo/Dordrecht, pp. 213–229.

Schmidt, U., Conrad, R., 1993. Hydrogen, carbon monoxide, and methane dynamics in Lake Constance. Limnol. Oceanogr. 38, 1214–1226.

Siegel, S., Hedgpeth, H., 1967. Chemistry of irradiation induced polytetrafluoroethylene radicals: I. Re-examination of the EPR spectra. J. Chem. Phys. 46, 3904–3912.

Thompson, A.M., 1992. The oxidizing capacity of the Earth's atmosphere: probable past and future changes. Science 256, 1157–1165.

Valentine, R.L., Zepp, R.G., 1993. Formation of carbon monoxide from the photodegradation of terrestrial dissolved organic carbon in natural waters. Environ. Sci. Technol. 27, 409–412.

Wiesenburg, D.A., Guinasso Jr., N.L., 1979. Equilibrium solubilities of methane, carbon monoxide, and hydrogen in water and sea water. J. Chem. Eng. Data 24 (4), 356–360.

Wilks, S.S., 1963. Toxic photooxidation products in closed environments. Aerosp. Med. 34, 838–841.

Xie, H., Zafiriou, O.C., Wang, W., Taylor, C.D., 2000. Distribution, production, and consumption of carbon monoxide in the Sargasso Sea (Poster OS31A-07). Trans. Am. Geophys. Union 80 (49), 144.

Xie, H., Zafiriou, O.C., Wang, W., Taylor, C.D., 2001. A simple automated continuous-flow-equilibration method for measuring carbon monoxide in seawater. Environ. Sci. Technol. 35, 1475–1480.